ELSEVIER

Earth and Planetary Science Letters 202 (2002) 741–752

EPSL

www.elsevier.com/locate/epsl

Probing the Pacific's oldest MORB glass: mantle chemistry and melting conditions during the birth of the Pacific Plate

Martin Fisk [a,*], Katherine A. Kelley [b]

[a] College of Oceanic and Atmospheric Sciences, Oregon State University, Corvallis, OR 97331, USA
[b] Department of Earth Sciences, Boston University, Boston, MA 02215, USA

Received 11 January 2002; received in revised form 14 May 2002; accepted 4 June 2002

Abstract

Major element chemistry of basalt from the southern East Pacific Rise (EPR) is different from that of the EPR at the time of the formation of the Pacific Plate at 170 Ma. Glass recovered from Jurassic age (170 Ma) Pacific ocean crust [Bartolini and Larson, Geology 29 (2001) 735–738] at Ocean Drilling Program Hole 801C records higher Fe_8 (10.77 wt%) and marginally lower Na_8 (2.21 wt%) compared to the modern EPR, suggesting deeper melting and a temperature of initial melting that was 60°C hotter than today. Trace element ratios such as La/Sm and Zr/Y, on the other hand, show remarkable similarities to the modern southern EPR, indicating that Site 801 was not generated on a hotspot-influenced ridge and that mantle composition has changed little in the Pacific over the past 170 Ma. Our results are consistent with the observation that mid-ocean ridge basalts (MORBs) older than 80 Ma were derived by higher temperature melting than are modern MORBs [Humler et al., Earth Planet. Sci. Lett. 173 (1999) 7–23], which may have been a consequence of the Cretaceous superplume event in the Pacific. Site 801 predates the formation of Pacific oceanic plateaus and 801C basalt chemistry indicates that higher temperatures of mantle melting beneath Pacific ridges preceded the initiation of the superplume.

Keywords: Jurassic; oceanic crust; mid-ocean ridge basalts; glasses; East Pacific Rise; major elements; trace elements; mantle; temperature

1. Introduction

The Pacific Plate was born when the East Pacific Rise (EPR) formed in the central Pacific Superocean, south of the magnetic equator at 170–175 Ma [1] (Fig. 1). This early Pacific crust, which is now in the western Pacific (Fig. 1), has been investigated twice by the Ocean Drilling Program (ODP). Leg 129 Hole 801B encountered basement at 462 m below the seafloor and was the first site to recover Jurassic ocean crust in the Pacific [3], and Hole 801C penetrated 129 m into basement (mib) rock. On returning to the site, ODP Leg 185 deepened Hole 801C to 470 m into igneous rock [4]. Ages of the rocks from Hole 801C basement were determined to be 165 Ma [5], which is similar to the initial age determination

* Corresponding author. Tel.: +1-541-737-5208.
E-mail address: mfisk@coas.oregonstate.edu (M. Fisk).

0012-821X/02/$ – see front matter
PII: S0012-821X(02)00760-4

for Leg 129 rocks of 170 Ma [6]. These dates place 801C very close to the time of the birth of the Pacific Plate based on paleomagnetic and paleontologic data [1].

Mid-ocean ridge basalts (MORBs) older than 80 Ma appear to have lower Na_2O than basalts from ocean ridges today, suggesting thicker crust and hotter ocean mantle in the past [2]. This may have been due to the rise of the Cretaceous superplume, which spawned oceanic plateaus in the Pacific. Hole 801C is a critical datum for the chemistry of ancient MORBs because it predates the formation of Pacific oceanic plateaus from 125 to 80 Ma related to the Cretaceous superplume event [7].

Chemical comparison of Cretaceous and older basalts with modern basalts is complicated by seafloor weathering of the old basalts. Primary igneous minerals are replaced with secondary, low-temperature minerals, and void spaces and fractures are filled with clays and other minerals, which result in changes in the composition of the whole rock. Unaltered basalt glass can accurately record the original basalt composition, and glass that experiences limited interaction with seawater can remain unaltered for millions of years. In Hole 801C, significant quantities of glass from the exteriors of basalts were preserved. These glasses allow us to examine how the EPR crustal composition and underlying mantle at 170 Ma differ from the present EPR. These 801C basalts along with modern EPR basalts span the full age of the Pacific Plate, and no significantly older seafloor glasses are likely to be found in the Pacific Basin. Hole 801C could reveal if hotter upper mantle existed back to 170 Ma, or if it was associated with the Cretaceous superplume in the Pacific.

2. Samples, methods and results

At Hole 801C, the upper 27 m of volcanic rocks are younger (157 Ma) and more alkalic than the lower units (165–170 Ma) [5,6,8]. The upper 27 m of basement is separated from the lower sections by a 20 m thick hydrothermal unit [9]. Below the hydrothermal unit is a 65 m thick zone of lava flows, which on the basis of its physical properties, structure and chemistry appears to have erupted off-axis [10] and is not necessarily representative of normal, fast-spreading oceanic crust. Below these off-axis basalts are basaltic pillows and flows, massive basalts, breccias and interflow hyaloclastites, all of which appear to be MORBs based on shipboard determinations of mineralogy and whole rock chemistry [4].

A layer of volcanic glass 1–2 cm thick forms on the exteriors of subaqeous lavas, because they are rapidly quenched by contact with seawater. Volcanic glass is metastable in seawater, but is not completely transformed to secondary minerals even in these 170 Ma basalts. Volcanic glass provides the truest indication of the composition of magmatic liquids because the microbeam techniques used to analyze glass can avoid included minerals and secondary alteration, both of which influence chemical analyses of whole rocks. A total of 36 glass samples were collected from every location where it was preserved at Hole 801C. (See Appendix for descriptions of glass containing units.) Some notable occurrences of glass were from chemically distinct lavas in Core 5 just below the hydrothermal unit, from zones of abundant glass (Cores 12, 23, 28 and 42) and from basalt associated with interflow sediment (Core 27).

Twelve-element electron microprobe analyses (Table 1) were acquired with a four-spectrometer CAMECA SX-50 at Oregon State University. Details of beam conditions, counting times and standards were published previously [11]. Thirty-six analyses of our internal standard (USNM 113498/1 VG-A99 [12]) were collected during the same analytical sessions as the 801C glasses. The precision of these analyses is indicated by the standard deviations of the 36 analyses (Table 1). The accuracy [(measured−accepted)/accepted, in percent] of seven major elements is within 1% of the accepted values (Table 1).

Five of the glasses from 801C were also analyzed for trace element chemistry (Table 2) by laser ablation inductively coupled plasma-mass spectrometry (ICP-MS) at Boston University, using a VG/Merchantek Microprobe II 213 nm laser ablation system coupled with a VG PQ ExCell

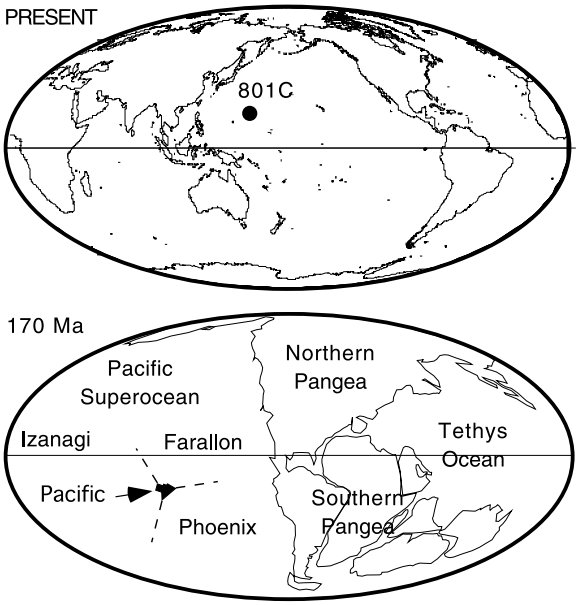

Fig. 1. (Top) Map locating ODP Hole 801C in the western Pacific. Hole 801C, 18°38.538′N, 156°21.588′E, 5674 m water depth. (Bottom) Plate reconstruction showing the location of the Pacific Microplate at 170 Ma [1,33].

quadrupole ICP-MS. Analyses were acquired using a 100 μm spot size, and time-resolved laser data were averaged over 30 s, background-subtracted and normalized to Ti as an internal standard. Trace element concentrations were calculated by calibrating with three USGS basalt glass standards (BHVO-2G, BCR-2G and BIR-1G) and ICP-MS solution data for picked chips of the same glasses. Repeat laser analyses show reproducibility of $<3\%$ relative standard deviation for Sr, Nb, Y and U. Comparison of the laser results to solution ICP-MS analyses of chips of the same glasses shows $<5\%$ difference between the two techniques for the same elements.

The smooth variations of MgO, CaO, FeO and P_2O_5 (Fig. 2A–C) as well as SiO_2, Al_2O_3, TiO_2 and K_2O (not shown) are consistent with the liquid line of descent of magmas experiencing crystallization. The chemical variations displayed by 801C basalts are the consequence of cooling of a basaltic magma reservoir in which olivine, plagioclase feldspar and clinopyroxene are crystallizing. Elements more abundant in the crystallizing assemblage than in the residual liquid are removed from the liquid (for example, CaO and MgO, which both decrease as crystallization proceeds, Fig. 2A). Elements less abundant in the crystallizing assemblage of minerals than in the residual silicate liquid (for example, FeO and P_2O_5, Fig. 2B,C) increase in the liquid as crystallization proceeds. A fractional crystallization model [13] shows the expected changes in MgO, CaO, FeO and Na_2O (Fig. 2A,B,D) as a result of crystallization of a magma with a composition equivalent to the glass found in Hole 801C Core 42 (Table 1).

Only the MgO–Na_2O variation diagram (Fig. 2D) does not support the hypothesis that all magmas are related by crystallization. Eight glasses with 5.9–6.7 wt% MgO have Na_2O that falls below the trend of the rest of the glasses from 801C and well below the MgO–Na_2O trend of the present day EPR. These low-Na_2O glasses could be from a separate magma system or could result from higher percentages of melting of the underlying mantle than the bulk of the basalts at this site. Both of these hypotheses seem unlikely, as only Na_2O deviates from the MgO trends. P_2O_5, K_2O, TiO_2 and incompatible trace elements should also deviate from linear MgO arrays in the same manner as Na_2O if mantle or magmatic processes were responsible for the eight low-Na_2O basalts. Yet P_2O_5, Zr, La (Fig. 2C,F,G) and other incompatible elements (not shown) form linear MgO-element arrays. This low Na_2O relative to P_2O_5 is demonstrated in Fig. 2E, where the Na_2O of the eight glasses falls to the left of other glasses from Hole 801C and also to the left of the field that contains EPR basalts.

We suggest that the low Na_2O of the eight glasses is an analytical artifact due to the hydration of these glasses by prolonged contact with water. In electron probe analysis the intensity of Na X-rays is known to decrease with time. This decay is more rapid in hydrous glass [14]. Ingrowth of Si and Al X-ray intensity occurs in some glasses as a consequence of sodium decay [15], which may account for the high totals for three of the low-sodium glasses (Table 1). The Hole 801C glasses affected by sodium loss therefore fall outside the field for glasses from 801C

Table 1
Major element chemistry of Hole 801C volcanic glass (wt%)

Sample[a]	mib[b]	*n*[c]	Na_2O	MgO	Al_2O_3	SiO_2	P_2O_5	S	K_2O	CaO	TiO_2	Cr_2O_3	MnO	FeO	Sum
129 801C 5 R 3 101 102 4A	***41.8***	***7***	***2.70***	***7.50***	***15.69***	***50.16***	***0.24***	***0.15***	***0.57***	***11.75***	***1.80***	***0.08***	***0.12***	***9.21***	***99.96***
129 801C 5 R 4 36 37 2B	***42.6***	***11***	***2.18***	***9.29***	***17.24***	***48.98***	***0.06***	***0.14***	***0.01***	***12.95***	***0.97***	***0.09***	***0.11***	***8.60***	***100.63***
129 801C 12 R 1 57 61 11	***94.9***	***9***	***2.71***	***6.24***	***13.02***	***49.89***	***0.17***	***0.21***	***0.13***	***10.98***	***2.31***	***0.01***	***0.15***	***13.61***	***99.43***
129 801C 12 R 1 75 79 13	***95.1***	***8***	***2.66***	***6.20***	***13.11***	***49.73***	***0.18***	***0.29***	***0.13***	***10.85***	***2.30***	***0.03***	***0.18***	***13.52***	***99.20***
129 801C 12 R 1 149 150 23	***95.8***	***9***	***2.68***	***6.28***	***12.95***	***49.45***	***0.17***	***0.21***	***0.12***	***10.91***	***2.29***	***0.01***	***0.19***	***13.41***	***98.67***
129 801C 12 R 2 21 28 2	***96.0***	***6***	***2.70***	***6.28***	***13.00***	***49.51***	***0.18***	***0.21***	***0.13***	***10.99***	***2.31***	***0.01***	***0.15***	***13.44***	***98.89***
185 801C 16 R 5 107 113 13	**137.0**	**11**	**2.42**	**5.89**	**12.99**	**49.41**	**0.29**	**0.29**	**0.19**	**10.49**	**3.06**	**0.02**	**0.22**	**15.28**	**100.57**
185 801C 17 R 3 85 91 6	143.6	9	2.67	6.05	12.63	49.44	0.21	0.22	0.15	10.59	2.65	0.01	0.20	14.48	99.28
185 801C 18 R 1 47 49 9	149.7	12	2.65	6.18	13.10	49.58	0.20	0.27	0.14	10.76	2.47	0.01	0.17	14.24	99.76
185 801C 22 R 3 7 14 2	183.4	12	2.60	6.64	13.33	49.82	0.16	0.21	0.14	11.06	2.13	0.01	0.18	12.81	99.10
185 801C 23 R 1 13 16 3A	**189.0**	**5**	**2.43**	**6.51**	**13.36**	**49.45**	**0.18**	**0.19**	**0.15**	**11.12**	**2.19**	**0.02**	**0.17**	**12.93**	**98.68**
185 801C 23 R 1 109 111 9	190.0	6	2.53	6.63	13.42	50.00	0.19	0.19	0.14	11.13	2.21	0.02	0.19	13.25	99.89
185 801C 23 R 3 50 55 4	**192.1**	**3**	**2.38**	**6.54**	**13.63**	**50.23**	**0.19**	**0.25**	**0.13**	**11.22**	**2.20**	**0.00**	**0.15**	**13.49**	**100.41**
185 801C 23 R 4 0 3 1	**193.0**	**3**	**2.45**	**6.68**	**13.81**	**50.45**	**0.16**	**0.27**	**0.14**	**11.37**	**2.25**	**0.00**	**0.16**	**13.88**	**101.61**
185 801C 24 R 1 90 92 10	199.2	6	2.68	6.56	13.29	49.51	0.16	0.26	0.13	11.09	2.19	0.03	0.16	13.25	99.31
185 801C 25 R 1 2 4 1A	207.7	9	2.59	6.82	13.70	49.75	0.15	0.24	0.11	11.32	2.10	0.04	0.18	13.12	100.12
185 801C 27 R 3 0 5 10 1	229.5	12	2.48	7.16	14.21	49.85	0.14	0.23	0.13	11.86	1.88	0.26	0.16	11.78	100.12
185 801C 28 R 1 88 102 2	236.6	9	2.43	7.14	14.03	49.52	0.14	0.23	0.13	11.69	1.84	0.32	0.16	11.52	99.14
185 801C 28 R 2 67 71 2	237.7	12	2.44	7.54	14.30	49.67	0.13	0.23	0.10	11.80	1.73	0.37	0.17	11.31	99.80
185 801C 28 R 2 118 122 9	238.2	9	2.42	7.44	14.40	49.80	0.14	0.23	0.12	11.97	1.72	0.37	0.16	11.41	100.17
185 801C 28 R 3 37 43 2	238.9	9	2.40	7.69	14.24	49.51	0.14	0.24	0.11	12.07	1.78	0.28	0.16	11.59	100.23
185 801C 28 R 3 53 58 4	239.1	12	2.44	7.86	14.29	49.55	0.13	0.22	0.11	11.80	1.70	0.24	0.17	11.32	99.83
185 801C 28 R 3 86 90 8	239.4	9	2.41	7.47	14.35	49.70	0.12	0.23	0.10	11.92	1.74	0.33	0.16	11.35	99.89
185 801C 28 R 3 90 93 9	239.4	12	2.46	7.60	14.49	49.69	0.14	0.28	0.11	12.02	1.75	0.27	0.15	11.51	100.46
185 801C 29 R 1 20 32 2	**254.1**	**6**	**2.16**	**6.34**	**13.21**	**49.46**	**0.19**	**0.36**	**0.13**	**10.98**	**2.49**	**0.15**	**0.19**	**13.75**	**99.41**
185 801C 34 R 2 70 73 2B	**294.2**	**6**	**2.34**	**6.39**	**13.09**	**49.16**	**0.20**	**0.32**	**0.15**	**10.68**	**2.43**	**0.04**	**0.17**	**13.89**	**98.88**
185 801C 34 R 3 104 106 6	**296.1**	**9**	**2.19**	**6.30**	**13.18**	**49.02**	**0.19**	**0.34**	**0.15**	**10.82**	**2.46**	**0.01**	**0.19**	**13.84**	**98.69**
185 801C 35 R 3 29 32 1	304.9	9	2.69	6.41	13.19	49.87	0.21	0.34	0.15	10.77	2.43	0.10	0.19	13.98	100.33
185 801C 35 R 4 63 74 2	306.8	3	2.65	6.30	13.18	49.77	0.19	0.35	0.14	10.71	2.42	0.05	0.19	13.84	99.79
185 801C 42 R 2 63 65 3	368.8	9	2.42	8.26	15.01	49.68	0.11	0.24	0.08	12.22	1.38	0.19	0.15	10.27	100.00
185 801C 42 R 2 100 106 7	369.2	9	2.36	8.16	15.19	49.53	0.10	0.24	0.08	12.42	1.36	0.35	0.15	10.08	100.02
185 801C 42 R 2 116 120 10	369.4	12	2.42	8.20	15.18	49.67	0.11	0.18	0.08	12.27	1.35	0.03	0.14	10.18	99.83
185 801C 46 R 1 45 51 3	405.5	9	2.56	6.83	13.43	49.71	0.17	0.23	0.14	11.41	2.02	0.02	0.19	12.92	99.62
185 801C 48 R 1 85 88 2D	**424.6**	**9**	**2.37**	**6.66**	**13.34**	**48.96**	**0.18**	**0.23**	**0.14**	**11.43**	**2.06**	**0.02**	**0.20**	**12.74**	**98.34**
185 801C 48 R 2 60 62 6	425.6	9	2.65	6.69	13.45	49.67	0.16	0.22	0.14	11.14	2.05	0.01	0.19	12.82	99.20
Standard VG99 (measured)	n.a.	36	2.64	5.07	12.49	50.96	0.43	0.02	0.83	9.23	4.03	0.02	0.20	13.29	99.21
Standard VG99 (accepted)[e]	n.a.	n.a.	2.66	5.08	12.49	50.94	0.42[d]	n.r.	0.82	9.30	4.06	n.r.	0.15	13.30	99.22
Standard VG99 precision[f]	n.a.	36	0.09	0.04	0.10	0.25	0.03	0.01	0.03	0.15	0.09	0.01	0.02	0.23	
Standard VG99 accuracy[g]	n.a.	36	−0.8	−0.1	0.0	0.0	3.4	n.a.	1.5	−0.7	−0.7	n.a.	31.	−0.1	

n.a., not applicable; n.r., not reported. Samples in bold italics are off-axis eruptions. Samples in bold plain text have low Na_2O, as discussed in the text.

[a] Leg, Hole, Core, Section, top cm, bottom cm, piece.

[b] mib, meters into basement.

[c] *n*, number of spot analyses.

[d] E. Jarosewich, personal communication.

[e] Smithsonian standard USNM 113498/1 VG-A99 [12].

[f] Standard deviation.

[g] (Measured standard−accepted standard)/(accepted standard) in %.

Table 2
Selected major and trace element chemistry of Hole 801C volcanic glass

Sample	MgO	CaO	Li	Sc	V	Cr	Co	Ni	Cu	Rb	Sr	Y	Zr	Nb	Ba	Hf	Ta	Pb
801C-12R1-57	6.67	11.40	7.93	47.3	453	78.0	48.0	35.6	80.4	1.53	130	59.5	178	4.27	15.8	4.36	0.306	0.492
801C-23R1-13	**6.96**	**11.60**	**6.04**	**46.2**	**431**	**115**	**45.7**	**60.1**	**70.4**	**1.70**	**116**	**51.8**	**151**	**4.62**	**18.7**	**3.88**	**0.301**	**0.474**
801C-28R2-118	7.87	12.63	6.44	45.4	350	229	43.2	61.1	71.4	1.10	104	37.5	106	3.11	15.5	3.08	0.234	0.380
801C-42R2-116	8.48	12.89	4.61	43.2	284	308	43.4	75.1	73.3	0.485	120	30.4	86.6	2.09	9.47	2.31	0.152	0.284
801C-46R1-45	7.12	11.89	7.19	46.6	406	133	46.1	58.8	76.0	1.46	117	48.0	139	3.78	17.3	3.61	0.260	0.438

	Th	U	La	Ce	Pr	Nd	Sm	Eu	Gd	Tb	Dy	Ho	Er	Yb	Lu	La/Sm_N	Ce/Sm_N	Sm/Yb_N
801C-12R1-57	0.209	0.0803	5.34	17.2	3.07	15.7	6.13	2.02	8.31	1.40	9.14	2.05	5.71	5.58	0.885	0.538	0.665	1.19
801C-23R1-13	**0.250**	**0.0922**	**5.03**	**15.9**	**2.70**	**14.2**	**5.10**	**1.79**	**7.37**	**1.21**	**7.96**	**1.79**	**4.97**	**4.90**	**0.795**	**0.609**	**0.739**	**1.13**
801C-28R2-118	0.179	0.0884	3.46	11.1	2.03	11.0	3.99	1.32	5.68	0.921	6.37	1.44	4.08	3.89	0.626	0.536	0.662	1.11
801C-42R2-116	0.111	0.0443	2.86	8.78	1.62	8.45	2.83	1.15	4.48	0.763	4.55	1.12	3.01	2.91	0.416	0.624	0.736	1.06
801C-46R1-45	0.200	0.0176	4.58	13.9	2.44	13.4	4.87	1.58	6.77	1.11	7.56	1.66	4.55	4.47	0.692	0.580	0.678	1.18

MgO and CaO in wt%. Other elements in parts per million, ppm. Sample designations. Hole 801C, core number with suffix R, section number, top of interval within section in cm. REE ratios normalized to the chondrite [32]. Sample in bold has low Na_2O.

and the EPR (Fig. 2D,E). We consider the 801C glasses that are within the EPR data fields to be unaffected by hydration.

One of the hydrated glasses (23R1-13-16) was analyzed for trace elements by laser ablation ICP-MS. Trace elements such as Rb and U are highly enriched in oceanic crust during seafloor alteration and thus are sensitive indicators of the degree of alteration. Glass 23R1-13-16 has the highest Rb concentration of the five glasses selected for laser work and also has slightly higher Rb/La, reinforcing the interpretation that the low-Na glasses have been altered. Most other trace elements in this glass appear to be unaffected by the hydration. The remaining four glasses (Table 2) have average Ba/Rb of 13.4 and average U/Th of 0.40, which are both typical of NMORB (Ba/Rb = 11.3, U/Th = 0.39) [16] and indicate that these glasses are indeed pristine.

In igneous rocks, the abundance of incompatible elements (those with higher concentrations in silicate melts than in the assemblage of coexisting minerals) is related to the amount of mantle melting and the amount of magma crystallization. In Hole 801C the incompatible elements P, Zr and La all vary by a factor of 2 (Fig. 2C,F,G, respectively), and this variation can be attributed to crystallization. The ratios of incompatible elements such as P_2O_5/TiO_2, La/Sm and Zr/Y are generally insensitive to crystallization and are constant for this site (Fig. 2C,F,G). Incompatible element ratios in basalts can be affected by the composition of the mantle and the amount of melting (F) it undergoes. But if $F > 0.10$ and relatively constant (± 0.02), then incompatible trace element ratios are relatively insensitive to F. If these conditions are met for 801C, then the constant trace element ratios imply that the mantle source was chemically invariant during the time that the 801C lavas were generated. This is supported by a nearly constant Zr/Y of 3.04 (± 0.14, 1σ, $n = 28$) from shipboard analyses of the minimally altered whole rocks from Hole 801C [4].

A trend to low Zr and low Zr/Y starting at about 120 mib [4,8] indicates that these basalts are affected by either a change in the composition of the mantle source or a relatively large change in melting conditions. The depth of the change in

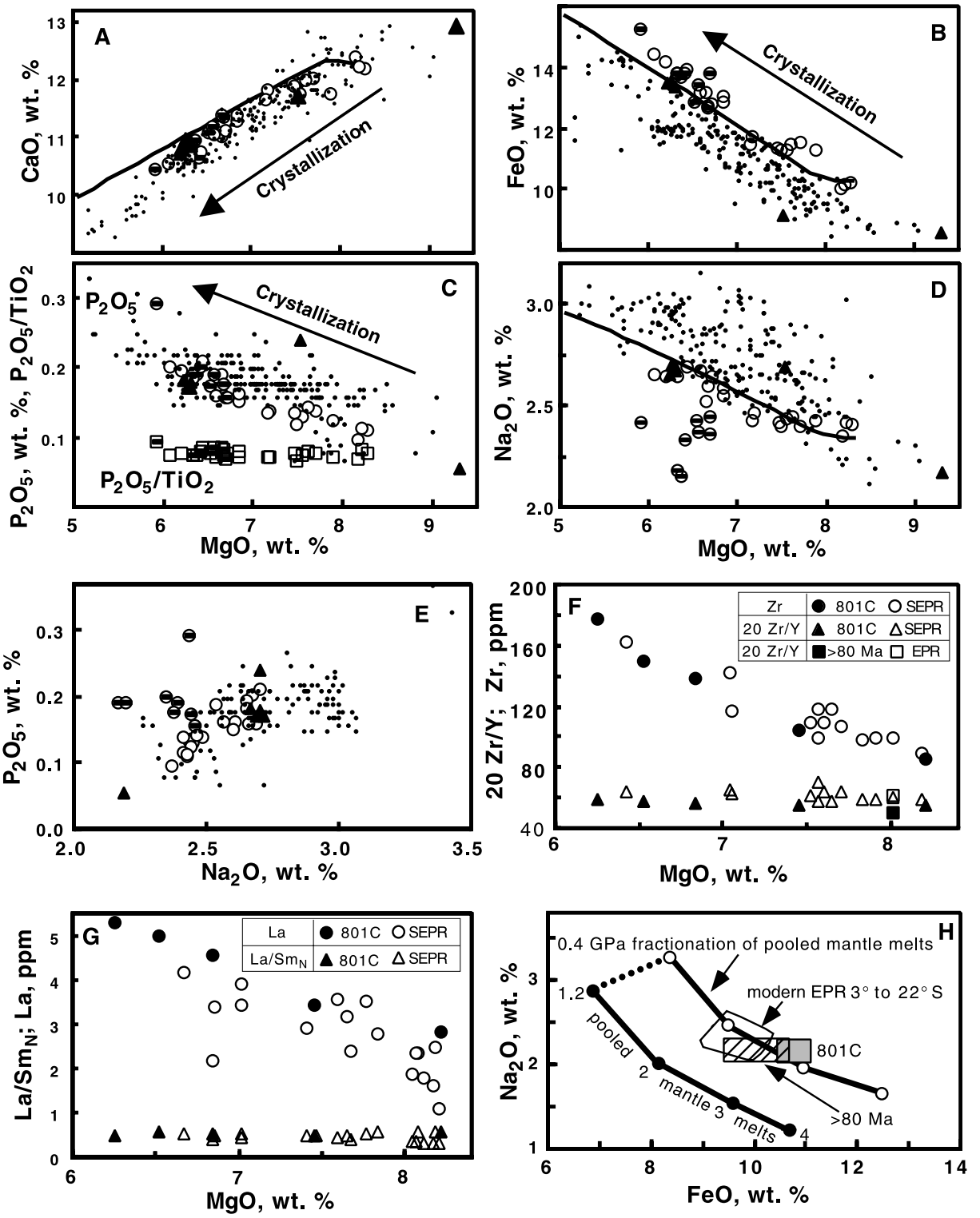
A
CaO, wt. %
Crystallization
B
FeO, wt. %
Crystallization
C
P2O5
Crystallization
P2O5/TiO2
P2O5, wt. %, P2O5/TiO2
MgO, wt. %
D
Na2O, wt. %
MgO, wt. %
E
P2O5, wt. %
Na2O, wt. %
F
Zr 801C SEPR
20 Zr/Y 801C SEPR
20 Zr/Y >80 Ma EPR
20 Zr/Y; Zr, ppm
MgO, wt. %
G
La 801C SEPR
La/SmN 801C SEPR
La/SmN; La, ppm
MgO, wt. %
H
0.4 GPa fractionation of pooled mantle melts
modern EPR 3° to 22° S
801C
>80 Ma
1.2
pooled mantle melts
2
3
4
Na2O, wt. %
FeO, wt. %

Table 3
Na_2O and FeO adjusted for crystallization

Source	Na_8[d] (wt%)	Na_8 (1 S.D.)[e]	Fe_8[d] (wt%)	Fe_8 (1 S.D.)
801C (this study)[a]	2.21	0.16	10.77	0.35
801C (this study)[b]	2.39	0.05	10.57	0.30
801C (this study)[c]	2.34	0.06	10.54	0.43
801C [2][f]	2.33	0.08	9.83	0.24
EPR 3–22°S (this study)	2.37	0.21	9.47	0.82
EPR regional average [2]	2.66	0.15	9.93	0.37
MORB >80 Ma [2]	2.20	0.18	9.98	0.63

[a] Klein and Langmuir model [24].
[b] Linear regression through 801C data projected to 8% MgO.
[c] Liquid line of descent model [13], projected to 8% MgO.
[d] Na_8 and Fe_8 defined [24].
[e] One standard deviation.
[f] The lower Fe_8 value derives from the newly acquired deep samples in this study and the use of whole rock chemistry in the previous study [2].

chemistry corresponds to a change in physical properties [10,17] and the upper 120 m of Hole 801C thus appears to be the product of off-axis volcanism. These lavas may not be representative of normal ridge volcanics and the glasses preserved within this sequence (Cores 5 and 12) were not included in comparisons of modern and ancient EPR basalt.

3. Discussion

For comparison to Hole 801C, we have selected 218 basalt glasses between 2°S and 23°S on the EPR for which major element data are available [18–21]. This section of the EPR was chosen because its present spreading rate is close to that of the calculated rate when Hole 801C formed (153 mm/yr) [1]. Today the spreading rate on the southern EPR is 150 ± 5 mm/yr from 3°S to 23°S [22,23].

Many of the major elements of the Hole 801C glasses fall within the chemical fields defined by young EPR basalts. Modern EPR glasses are, for example, indistinguishable from 801C in terms of CaO and MgO (Fig. 2A). This implies similar

←
Fig. 2. (A–D) Selected MgO variation diagrams for Hole 801C basalt glass. Triangles are 801C Cores 5 and 12 and are the basalts that erupted off-axis. Open circles and circles with bars are 801C Cores 16–48. Circles with bars are the eight samples that have low Na_2O as discussed in the text. Dots are present day basalts from the EPR from 3° to 22°S. Solid lines are the calculated chemical changes in a magma as a consequence of crystallization [13]. Arrows indicate the compositional changes expected for a cooling and crystallizing magma. (A) CaO vs. MgO. (B) FeO vs. MgO. Iron is total iron as FeO. (C) P_2O_5 vs. MgO. Squares are the ratios of P_2O_5 to TiO_2 in wt%. (D) Na_2O vs. MgO. The samples indicated by circles with bars appear to have low Na_2O as a consequence of glass hydration. (E) P_2O_5 vs. Na_2O. Low sodium is not associated with lower incompatible elements such as phosphorus. Same symbols as (A–D). (F) Zr and $20\times$Zr/Y vs. MgO. 801C samples are solid and modern EPR basalts between 6° and 22°S are open symbols. Modern data [25]. Squares are modern EPR and >80 Ma basalts [2]. (G) 801C La, circles, and La/Sm, triangles. Solid symbols are new analyses and open symbols are existing whole rock and glass analyses determined by X-ray fluorescence and ICP-MS [25,26]. (H) Na_2O vs. FeO of mantle melts and magmas evolved from these melts by fractional crystallization, and Fe_8 and Na_8 of three groups of basalts. Heavy solid line with dots at 1.2, 2, 3 and 4 is the pooled mantle melts at 1.2–4 GPa where melting is 50% fractional melting and 50% equilibrium melting [13]. The solid line with open circles is the locus of magmas with 8% MgO derived from mantle melts by crystallization at 0.4 GPa. The dotted line shows the evolution of one of the pooled melts (1.2 GPa) to a magma with 8 wt% MgO at 0.4 GPa. The three fields are the Na_8 and Fe_8 of modern EPR glasses from 3° to 22°S, no hatch; >80 Ma basalts [2], diagonal hatch; and the 801C basalts, gray. The sizes of the >80 Ma and 801C boxes represent the standard deviation of the Na_8 and Fe_8 values.

parent magma compositions and it also implies similar pressures (depths) of crystallization for the two populations. Pressure affects the temperature of the first appearance of calcic pyroxene, which results in lower CaO at similar MgO for magmas that crystallize at high pressure compared to those that crystallize at low pressure [13]. Other elements, such as P_2O_5 (Fig. 2C), TiO_2 and K_2O (not shown), are also similar in the present EPR and in 801C. Some 801C major elements, such as Na_2O (Fig. 2D), SiO_2 and Al_2O_3 (not shown), are shifted to the lower edge of the field of values for the EPR. In contrast to those elements, FeO is above the field of EPR basalt glasses (Fig. 2B).

Interlaboratory biases of microprobe data have been documented for some elements [11,13], but these biases would not account for the differences between modern and ancient Pacific basalts as documented here. The southern EPR glasses were analyzed by electron microprobe at the University of Hawaii and the Smithsonian Institution, both of which use the same internal glass standard (A99) as is used at Oregon State University [18–21]. This common internal glass standard (A99) [12] for all major element analyses in Fig. 2 indicates an internal consistency of these glass analyses, and that a real difference exists between old and young EPR MORB major element chemistry.

3.1. Fe_8

Total iron (FeO) in a basalt that has been adjusted to account for fractional crystallization has been termed Fe_8 [24]. Applying this adjustment to 801C basalt glasses gives an Fe_8 value of 10.77 ± 0.35 wt% (Table 3, Fig. 2H). Alternative methods of estimating Fe_8 are to apply a linear regression to the data and to calculate a liquid line of descent for the basalts [13]. Linear regression gives an Fe_8 of 10.57 ± 0.30 (Table 3), the liquid line of descent gives a similar Fe_8 value of 10.54 wt% for 801C basalts. The similarity of these three calculations indicates that the high Fe_8 value of these samples is not an artifact of the method of calculation. To be consistent with previous studies we use the Fe_8 value of 10.77 for comparisons. The Fe_8 of 801C glass is higher than all but four of the Fe_8 values for ocean ridges except those close to Iceland [24] and it is higher than the present EPR.

The deepest ocean rifts have Fe_8 values of 7.5 wt% and the shallowest ridges typically have $Fe_8 = 11.5$ wt% (excluding those affected by hotspots). The Fe_8 for the present EPR from 3° to 22°S is 9.47 ± 0.82 wt%. This present day lower Fe_8 on the southern EPR suggests a significant change in the generation of MORBs on the EPR between 170 Ma and the present. The value of Fe_8 for basalts older than 80 Ma is 9.98 wt% [2], which is between that of the present southern EPR and the 170 Ma EPR values (Fig. 2H).

If we assume that the composition of the mantle that generates southern EPR basalts has remained constant for the past 170 Ma, then the differences in Fe_8 can be interpreted in terms of changing melting conditions, since Fe_8 is relatively insensitive to F but will increase with increasing pressure of mantle melting. The compositions of pooled melts and their crystallization products (Fig. 2H) suggest that 'zero age' EPR basalts are the result of lower pressures of melting than 170 Ma EPR basalt. This shift in Fe_8 can be interpreted as a change in the depth of initial melting (P_0) of -0.5 GPa, for example from 2.8 GPa for 801C to 2.3 GPa for the modern EPR (Fig. 2H). These values are based on the projection of the centers of the 801C and EPR fields in Fig. 2H to the pooled mantle melts line. This change in P_0 corresponds to a decrease in the initial temperature of melting (T_0) of 60°C from 170 to 0 Ma, assuming that the slope of the solidus (dT_0/dP_0) is 120°C/GPa [24]. The decrease in T_0 from 170 Ma to the present is consistent with the conclusion (based on whole rock chemistry [2]) that the initial temperature of mantle melting today beneath ocean ridges is 50°C less than it was >80 Ma [2]. The decrease in P_0 and T_0 corresponds to a decrease in the average fraction of melting from 0.12 to 0.09, which is based on the relationship between the average extent of melting and P_0 when P_0 is greater than 0.8 GPa [24].

The difference in Fe_8 of ancient and modern EPR glasses could also be caused by different mantle compositions. As discussed below, how-

ever, the trace elements suggest that the present and 170 Ma EPR basalts are chemically similar.

3.2. Na_8

In a manner similar to calculating Fe_8, the Na_8 value of a basalt is obtained by applying a linear correction to the Na_2O wt% of the basalt as a function of MgO [24]. Applying the linear correction to the Na_2O and MgO of 801C basalts results in a value of Na_8 of 2.21 ± 0.16 wt%. In calculating Na_8 we have excluded the eight samples which we suspect are hydrated and thus appear to have anomalously low Na_2O, and we excluded the off-axis samples (Cores 5 and 12). The Na_8 of 801C is lower than most Pacific, Indian and South Atlantic regional averages [24]. For >80 Ma basalts, Humler et al. [2] obtained a nearly identical value of 2.20 ± 0.18 wt% Na_8 (Table 3).

Alternative methods of calculating Na_8 give values of 2.39 ± 0.05 for linear regression, and 2.34 ± 0.06 for liquid line of descent (Table 3). These Na_8 values are higher than the 2.21 value derived from the linear correction [24] and are the same as the present southern EPR and the >80 Ma basalts (Table 3). Thus although the linear correction gives a higher Na_8 for the present southern EPR than 801C, this is not a robust result. There appears to be a slight increase in Na_8 from 170 Ma to the present but this increase may not be significant. We note that the Na_8 value of 2.66 [2] for the northern EPR is much higher than the southern EPR and may reflect differences in spreading rate.

Shallow ocean rifts (1000 m water depth) have Na_8 of 1.75 wt%, and the deepest rifts (5000 m) have Na_8 of 3.25 wt%. If we accept that the subtle difference between ancient Na_8 (2.21) and modern Na_8 (2.37) on the southern EPR is the consequence of changes in melting conditions and that the mantle composition has remained constant, then increasing Na_8 with time (Fig. 2H) reflects decreasing F with time. A change in F from 0.12 to 0.09 (as mentioned above) would result in a small increase in the amount of Na_2O in the melt, because Na behaves as a mildly incompatible element. This change in F is compatible with the difference in crustal thickness from 6.8 km at Hole 801C [3] to an average of 5.5 km on the southern EPR [25].

Changes in mantle composition or the proportions of minerals could also affect Na_2O. If the abundance of clinopyroxene in the mantle varied from 17 to 22%, then the same 0.2 wt% increase in Na_2O would occur if F remained constant at 0.10 [13]. These compensating factors make interpretation of the Na_8 difficult and it appears that the major elements cannot resolve whether the change in basalt composition over time is a consequence of changing mantle composition or changing melting conditions. Trace elements, on the other hand, provide a means for distinguishing these two processes.

3.3. Trace elements

There is a large degree of along-axis geochemical variation on the modern EPR. We chose a segment of the EPR from 3° to 23°S because of its comparable spreading rate to that which generated the sequence at Site 801. The EPR from 8° to 15°N (used by Humler et al. [2] for comparison to >80 Ma basalts) is quite different from the EPR between 3° and 23°S in terms of Na_8, Zr/Y and Sm/Yb_N. The trace element concentrations and ratios of 801C glasses are, however, remarkably similar to those of the modern superfast-spreading portion of the EPR (Fig. 2F,G). These two data sets were collected by different methods; the modern MORB trace element data were determined by ICP atomic emission of glass separates [26] and by solution-based ICP-MS of whole rocks [27], whereas the ancient glasses were analyzed by laser ablation ICP-MS (this study) and solution ICP-MS (not reported). While our data suggest that no intralaboratory bias exists between laser ablation and solution ICP-MS data, there is no interlaboratory calibration between the modern and ancient trace element data sets.

Incompatible trace element ratios such as Zr/Y or La/Sm can reflect subtle differences in mantle melting when the fractions of melting are small (0.01–0.05). If, on the other hand, melt fractions are larger (for example, 0.09–0.12), the trace element ratios are relatively insensitive to small changes in F. Based on Fe_8, the melt fractions

that generated Site 801 and modern southern EPR basalts are in the range of 0.09–0.12. This range would have had an effect on Zr/Y and La/Sm that is less than the standard deviation of our analyses from 801C. Thus, Zr/Y and La/Sm suggest that the change in F over 170 Ma was not enough to cause significant variations in the trace element ratios, and that the two mantles are chemically similar within the precision of our analyses.

Larger amounts of melting of the same mantle source would result in a decrease in the incompatible trace element concentrations if all other conditions remained the same. The effect of melting at higher pressures (with temperature and composition held constant) is to increase incompatible elements, such as the La, Sm and Y, due to the lowering of the partition coefficients of these elements as pressure increases [28]. Thus, the larger extent of melting inferred by lower Na_8 and the higher pressure of melting inferred by Fe_8 of 801C basalts will have had compensating effects on the trace element abundance. The partition coefficient for Na_2O, on the other hand, increases with increasing temperature and pressure [13] so melting at greater depths and higher temperatures would result in lower Na_2O but higher La, Sm and Y.

Major and trace elements in MORBs are sensitive indicators of the proximity of an ocean ridge to mantle plumes [29]. The elevated Fe_8 and lower Na_8 of 801C basalts could be interpreted as the consequence of the influence of a mantle plume, if a plume was near the EPR 170 Myr ago. The absence of an oceanic plateau in the region of 801C argues against this, but the plateau could have been on the adjacent Phoenix, Farallon or Izanagi Plate (Fig. 1) and therefore not preserved. Plume-influenced ridge segments, however, are characterized by Nb and light rare earth enrichment, but the 801C basalts are depleted in light rare earth elements (Table 2) and have average Nb/Th of 18.8, typical of NMORB ($Nb/Th_{NMORB} = 19.4$) [16]. Mantle plume chemical discrimination diagrams such as that of Humler et al. [2] also indicate that 801C basalts were not close to a mantle plume, and we conclude that the different chemical characteristics of the 170 Ma and the present southern EPR are not a consequence of plume influence.

If deeper melting is responsible for the shift in Fe_8 erupted at 170 Ma, one might expect to see geochemical evidence of the involvement of garnet in the source. Garnet has a strong affinity for the heavy rare earth elements such as Yb, so the presence of residual garnet in the mantle source of ocean island basalts causes Sm/Yb_N to be greater than one in the resultant melt. The influence of garnet, however, is not observed in modern MORBs, even in localities such as Iceland [30], where melting clearly initiates within the garnet stability field. Our data thus do not resolve whether garnet may have been involved in the melt generation of these 170 Ma MORBs.

3.4. Global and regional significance

Trace elements appear to indicate that the mantle composition beneath the southern EPR is the same as that which produced the Hole 801C basalts, thus we do not think that the higher Fe_8 at 801C is due to different mantle composition. An alternative cause of higher P_0 (and Fe_8) in the past is higher water content of the mantle. The lavas at Site 801, however, show no indication of volatile contents higher than at ridges today. The lavas are not abnormally vesicular, there is no geochemical evidence (such as high Al_2O_3) to suggest high water content of the magmas, and the sum of the oxides from the microprobe analyses is close to 100% when calibrated against anhydrous basalt glass.

An alternative cause of higher P_0 is increased mantle temperature in the past, and the lower Na_8 prior to 80 Ma has been interpreted as a 50°C higher mantle temperature globally [2]. This higher temperature was not associated with higher P_0 because the data compilation did not reveal a higher Fe_8 before 80 Ma. Our result of a 60°C higher temperature of melting (T_0) at a single location (Site 801) is a consequence of the high P_0 and does not imply a globally higher temperature at 170 Ma, but could reflect a locally higher geotherm at the time of the birth of the Pacific Plate. The maximum thermal variations along modern spreading ridges are on the order of 70–150°C

[31] and the temperature difference we observe (60°C) between 801C and the present southern EPR is less than this.

4. Conclusions

Fresh basalt glass is preserved in the oldest Pacific Ocean crust yet recovered (ODP Hole 801C), which seems remarkable considering the high susceptibility of glass to alteration under most geologic conditions. These glasses record the composition of the nascent EPR shortly after the formation of the Pacific Plate at 170 Ma. The rate of spreading on the early EPR was similar to rates observed today in the region of the EPR between 3° and 22°S. Basalts from this segment of the EPR have lower FeO and slightly higher Na_2O (at similar MgO contents) than did the EPR 170 Myr ago. These temporal differences are consistent with a shift to a smaller fraction of melting of the mantle, shallower melting and lower initial temperature of melting over the last 170 Ma. The two end points in basalt chemistry (170 and 0 Ma) are clearly different, particularly in Fe_8, which implies differences in either mantle composition or melting conditions. Trace element data show that mantle composition has not changed significantly over the last 170 Ma and we conclude that the relatively high Fe_8 of Hole 801C basalts was the consequence of a higher mantle geotherm than is presently found along the southern EPR. A similar conclusion for globally distributed MORBs >80 Ma was reached based on Na_8 rather than Fe_8 [2]. Our data indicate that the higher temperature (and higher pressure) of initial melting at the birth of the Pacific Plate was within the normal variations of mantle temperature today and does not require a globally higher mantle temperature in the Jurassic. Glass chemistry from ODP sites that span the 170–80 Ma period [2] could reveal if deeper melting was a global phenomenon in this time interval.

Acknowledgements

We thank Roger Larson for discussions of age and paleo-spreading rates; Rob Pockalny for thoughts on crustal structure, modern ridge analogs and Hole 801C sample depths; Terry Plank for extensive and thoughtful reviews of early versions of the manuscript; Roger Nielsen for help with microprobe analyses and sample processing; and David Christie and Robert Duncan for discussions of mantle melting. The manuscript was greatly improved by comments from David Graham and three external reviewers: Wolfgang Bach, Jennifer Reynolds and Eric Humler. ODP Leg 185 chief and staff scientists, Terry Plank, John Ludden and Carlota Escutia; and the Leg 185 shipboard scientists, technicians, rig operators and crew all provided essential assistance. The Joint Oceanographic Institutions U.S. Science Support provided funds for this study. *[SK]*

Appendix

At Hole 801C chemically distinct glass from immediately below the alkalic section (157 Ma) was found in Core 5. All other glass was from the deeper (165–170 Ma) ocean ridge basalts. Four glasses from Core 12 are from within a 1.2 m interval of lava pillows and flows (Table 1). Glass was preserved in a breccia 168 mib and on pillow lava rims at three locations from 175.0 to 214.8 mib. Within the short interval 220.4–224.4 mib glass is preserved at four locations on the margins of pillows and flows. At 230.6 and 239.1 mib glass is found on pillow margins. In Core 27 at 260.9 mib glass is found in a hyaloclastite associated with sediment just above a 7 m thick flow. Closely spaced concentrations of glass were found in hyaloclastite breccias and interpillow material in the 2.8 m interval from 268.0 to 270.8 mib. Glass in Core 29 is from the top of a 14 m thick flow. Below the glassy pillow basalt units at 325.6–327.5 mib and 336.3–338.2 mib there is a 60 m interval in which no glass is preserved. At 400.2–400.6 mib abundant glass is preserved in a hyaloclastite. Core 46 recovered a glass chill margin at the base of a 7.5 m thick flow. The deepest glass recovered (456–457 mib) is from a pillow basalt and the base of a thin flow in Core 48.

References

[1] A. Bartolini, R.L. Larson, Pacific microplate and the Pangea supercontinent in the Early to Middle Jurassic, Geology 29 (2001) 735–738.

[2] E. Humler, C. Langmuir, V. Daux, Depth versus age: new perspectives from the chemical composition of ancient crust, Earth Planet. Sci. Lett. 173 (1999) 7–23.

[3] Y. Lancelot, R. Larson et al., Proc. ODP, Init. Repts. 129, College Station, TX, 1990, 488 pp.

[4] T. Plank, J.N. Ludden, C. Escutia et al., Proc. ODP, Init. Repts. 185 (2000) [CD-ROM]. Available from: Ocean Drilling Program, Texas A&M University, College Station, TX.

[5] A.A.P. Koppers, H. Staudigel, R.A. Duncan, High resolution $^{40}Ar/^{39}Ar$ dating of the oldest oceanic crust in the western Pacific Ocean (2002) in preparation.

[6] M.S. Pringle, Radiometric ages of basaltic basement recovered at Sites 800, 801, and 802, Leg 129, western Pacific Ocean, in: R.L. Larson, Y. Lancelot et al. (Eds.), Proc. ODP, Sci. Results 129, College Station, TX, 1992, pp. 389–404.

[7] R.L. Larson, Latest pulse of Earth: evidence for a mid-Cretaceous superplume, Geology 19 (1991) 547–550.

[8] P.A. Floyd, P.R. Castillo, Geochemistry and petrogenesis of Jurassic ocean crust basalts, Site 801, in: R.L. Larson, Y. Lancelot et al. (Eds.), Proc. ODP, Sci. Results 129, College Station, TX, 1992, pp. 361–388.

[9] R.L. Larson, A.T. Fisher, R.D. Jarrard, K. Becker ODP Leg 144 Shipboard Scientific Party,, Highly permeable and layered Jurassic oceanic crust in the Western Pacific, Earth Planet. Sci. Lett. 199 (1993) 71–83.

[10] R.A. Pochalny, R.L. Larson, Implications for crustal accretion at fast-spreading ridges from observations in Jurassic oceanic crust in the western Pacific, Geochem. Geophys. Geosyst., submitted.

[11] M.R. Fisk, A.W. McNeill, D.A. Teagle, H. Furnes, W. Bach, Major element chemistry of Hole 896A glass: data report, in: J. Alt, H. Kinoshita et al. (Eds.), Proc. ODP, Sci. Results 148, College Station, TX, 1996, pp. 483–487.

[12] E. Jarosewich, J.A. Nelen, J.A. Norberg, Reference samples for electron microprobe analyses, Geostand. Newsl. 4 (1990) 43–47.

[13] C.H. Langmuir, E.M. Klein, T. Plank, Petrologic systematics of mid-ocean ridge basalts: constraints on melt generation beneath ocean ridges, in: J.P. Morgan, D.K. Blackman, J.M. Sinton (Eds.), Mantle Flow and Melt Generation at Mid-Ocean Ridges, Geophys. Monogr. 71, 1992, pp. 183–280.

[14] C.H. Nielsen, H. Sigurdsson, Quantitative methods for electron microprobe analysis of sodium in natural and synthetic glasses, Am. Mineral. 66 (1981) 547–552.

[15] G.B. Morgan VI, D. London, Optimizing the electron microprobe analysis of hydrous alkali aluminosilicate glasses, Am. Mineral. 81 (1996) 1176–1185.

[16] S.-S. Sun, W.F. McDonough, Chemical and isotopic systematics of oceanic basalts: implications for mantle composition and process, in: A.D. Saunders, M.J. Norry, (Eds.), Magmatism in the Ocean Basins, Geol. Soc. Spec. Publ. 42, 1989, pp. 313–345.

[17] L.J. Abrams, R.A. Pockalny, R.L. Larson, K. Kelley, A model for the temporal emplacement of oceanic crust at Hole 801C, EOS Trans. AGU Fall Meet. 82 (Suppl.) (2001) F1147.

[18] L.S. Hall, J.M. Sinton, Geochemical diversity of the large lava field on the flank of the East Pacific Rise at 8 degrees 17′S, Earth Planet. Sci. Lett. 142 (1996) 241–251.

[19] J.M. Sinton, personal communication, 2001.

[20] J.M. Sinton, S.M. Smaglik, J.J. Mahoney, K.C. Macdonald, Magmatic processes at superfast spreading mid-ocean ridges: glass compositional variations along the East Pacific Rise 13°–23°S, J. Geophys. Res. 96 (1991) 6133–6155.

[21] W.G. Melson, T. O'Hearn, personal communication, 2001.

[22] C. DeMets, R.G. Gordon, D.F. Argus, S. Stein, Effect of recent revisions to the geomagnetic reversal time scale on estimate of current plate motions, Geophys. Res. Lett. 21 (1994) 2191–2194.

[23] D.F. Naar, R.N. Hey, Recent Pacific-Easter-Nazca plate motions, in: J.M. Sinton (Ed.), Evolution of Mid Ocean Ridges, Am. Geophys. Union Geophys. Monogr. 57, 1989, pp. 9–30.

[24] E.M. Klein, C.H. Langmuir, Global correlations of ocean ridge basalt chemistry with axial depth and crustal thickness, J. Geophys. Res. 92 (1987) 8089–8115.

[25] J.P. Canales, R.S. Detrick, S. Bazin, A.J. Harding, J.A. Orcutt, Off axis crustal thickness across and along the East Pacific Rise within the melt area, Science 280 (1998) 1218–1221.

[26] W. Bach, E. Hegner, J. Erzinger, M. Satir, Chemical and isotopic variations along the superfast spreading East Pacific Rise from 6 degrees to 30 degrees S, Contrib. Mineral. Petrol. 116 (1994) 365–380.

[27] R. Hekinian, R.D. Bideau, R. Hebert, Y. Niu, Magmatism in the Garrett Transform Fault (East Pacific Rise near 13 degrees 27′S), J. Geophys. Res. 100 (1995) 10163–10185.

[28] P.J. Hack, R.L. Nielsen, A.D. Johnston, Experimentally determined rare-earth and Y partitioning behavior between clinopyroxene and basaltic liquids at pressures up to 20 kbar, Chem. Geol. 117 (1994) 89–105.

[29] J.-G. Schilling, Iceland mantle plume geochemical study of the Reykjanes Ridge, Nature 242 (1973) 565–571.

[30] L. Slater, D. McKenzie, K. Gronvold, N. Shimizu, Melt generation and movement beneath Theistareykir, NE Iceland, J. Petrol. 42 (2001) 321–354.

[31] D.L. Anderson, The scales of mantle convection, Tectonophysics 284 (1998) 1–17.

[32] N. Nakamura, Determination of REE, Ba, Fe, Mg, Na and K in carbonaceous and ordinary chondrites, Geochim. Cosmochim. Acta 38 (1974) 757–775.

[33] M.F. Coffin, L.A. Lawver, L.M. Gahagan, D.A. Campbell, The Plates Project 2000 Atlas of Plate Reconstructions (750 Ma to Present Day), University of Texas, Austin, TX, Plates Project Progress Report 250, 2000, 89 pp.